Int. J. Electrochem. Sci., 15 **(2020)** 12173 – 12191, doi: 10.20964/2020.12.01

International Journal of
ELECTROCHEMICAL
SCIENCE
www.electrochemsci.org

Mechanical features of copper coatings electrodeposited by the pulsating current (PC) regime on Si(111) substrate

Ivana O. Mladenović[1], *Jelena S. Lamovec*[2], *Dana G. Vasiljević Radović*[1], *Vesna J. Radojević*[3] *and Nebojša D. Nikolić*[1,*]

[1] University of Belgrade, Institute of Chemistry, Technology and Metallurgy, Njegoševa 12, 11 000 Belgrade, Serbia
[2] University of Criminal Investigation and Police Studies, Cara Dušana 196, Zemun, 11 000 Belgrade, Serbia
[3] University of Belgrade, Faculty of Technology and Metallurgy, Karnegijeva 4, 11 000 Belgrade, Serbia
[*]E-mail: nnikolic@tmf.bg.ac.rs

Received: 8 August 2020 / *Accepted:* 26 September 2020 / *Published:* 31 October 2020

Mechanical features of the Cu coatings produced by the pulsating current (PC) regime on Si(111) substrate have been investigated. The Cu coatings were electrodeposited by varying duty cycle (15–50 %) and keeping the current density amplitude constant (100 mA cm^{-2}), and by keeping duty cycle constant (50 %) but varying the current density amplitude value (80–120 mA cm^{-2}). The scanning electron microscopy (SEM) and optical microscopy (OM) techniques showed that morphology of the coatings changed with increasing the duty cycle from those with large and well defined grains to uniform and compact fine-grained coatings. The Vickers microindentation technique was used for an examination of hardness applying the Chen-Gao (C-G) composite hardness model and indentation creep features of the Cu coatings. The obtained values of hardness for the Cu coatings on Si(111) in the 0.9069–1.5079 GPa range indicated the successful implementation of the C-G model for this „soft film on hard substrate“ composite system. The obtained stress exponents ranging from 2.79 to 5.29 indicated that creep mechanism changed from grain boundary sliding to both dislocation climbs and dislocation creep with decreasing duty cycle values. The maximum hardness and minimum stress exponent was obtained for the fine-grained Cu coating produced with a duty cycle of 50 % and the current density amplitude of 100 mA cm^{-2}, indicating that its plastic deformation during microindentation was primarily caused by grain boundary sliding. Optimization of process formation and mechanical features of the Cu coatings was made using Response Surface Methodology (RSM), and error of 3.2 % showed a good agreement between predicted and measured values.

Keywords: copper; pulsating current (PC); hardness; stress exponent; response surface methodology (RSM).

1. INTRODUCTION

Copper in the form of thin films or uniform compact coatings formed on various substrates found wide application in many important technologies including micro-electro-mechanical systems (MEMS) [1, 2], micro-opto-electro-mechanical systems (MOEMS) [3], microelectronic packaging and interconnects [4]. Various processes, such as chemical vapour deposition (CVD), physical vapour deposition (PVD), electrodeposition (ED) and electroless deposition (EL), are used to obtain copper for the above mentioned applications [5].

Among all methods of coating formation, electrodeposition technique represents especially suitable method to obtain uniform and compact metal coatings. The advantage of this method in relation to all other methods is an easy control of thickness of coatings and obtaining of coatings of desired features by a choice of regimes and parameters of electrolysis [6]. Comparing constant and pulse regimes of electrodeposition, certain advantages in a quality (i.e. morphological and structural features) of the coatings like lower porosity and fine-grained structure are realized by application of pulse electrodeposition processes [6, 7]. Regarding copper electrodeposition processes, the parameters applied in both constant and pulse electrodeposition processes affecting a quality of the coatings are stirring of electrolyte [8–10], the presence of additives in electrolytes [11–15], composition and temperature of electrolytes [6, 10], etc. Various types of substrate, such as stainless steel [16], nickel coatings [17] and silicon [18], are among the most often used substrates in copper electrodeposition processes.

The hardness represents one of the most important mechanical features of coatings [19]. Hardness of coatings can be determined directly using small indentation load test (case I: thicker film and a slight impact of the substrate hardness) or indirectly using a composite hardness model approach for a determination of true hardness of the film (case II: thin films and a greater contribution to substrate hardness in the value of measured composite hardness) [20].

The composite hardness represents complex function of many factors which include contributions of both the substrate hardness and the coating hardness in the measured hardness value. To extract a true value of the coating hardness from the composite hardness measurements, several composite hardness models have been developed [21–23]. The composite hardness models have been already used for a determination of copper film hardness [24], and it was found [9, 18, 25–27] that hardness of the Cu coatings strongly depended on their morphological and structural features. For a determination a true hardness of Cu films and coatings, different composite hardness models have been applied, and some of them [28–31] give very good fits to experimental data with real obtained values of hardness of both the substrate and the coating. The choice of composite hardness models depends on many factors like composite system type, thickness of coating, choice of measurement methods, etc.

The indentation creep method represents a quick, simple and non-destructive method for an investigation of mechanical features of various composite systems. The main aim of application of this method is an obtaining information related with the time dependent flow of materials, i.e. determination of the creep resistance of metal coatings [32]. The investigation of the creep behavior of the composite systems is essential to evaluate a mechanical reliability, especially when nanodevices are used under long term stress conditions or for fabricated low-dimensional piezoelectric devices [33,

34]. This method is also applied in examination of Cu coatings used in the design of nuclear fuel containers for deep geological repositories, since Cu coatings are suitable as long-lived barrier with satisfactory degree of corrosion resistance [35].

In this study, hardness of Cu coatings formed by pulse electrodeposition with various duty cycles on Si(111) substrate has been determined by application of Chen-Gao composite hardness model. Simultaneously, the indentation creep method is used to investigate the power low indentation creep features of the Cu coatings obtained under the same electrodeposition conditions. The creep resistance of the Cu coatings was determined in this way.

Also, prediction and optimization of the composite hardness of the Cu coatings was done by varying both electrodeposition parameters and applied indentation load using RSM (Response Surface Methodology) method [36, 37]. The mutual interactions between three variables (duty cycle, thickness of Cu coatings and applied indentation load) were analyzed.

2. EXPERIMENTAL

The copper coatings were produced via electrodeposition route using the pulsating current (PC) regime. For that purpose, an electrolyte containing 240 g L^{-1} $CuSO_4 \cdot 5\ H_2O$ in 60 g L^{-1} H_2SO_4 was used. The parameters of the PC regime used for a formation of compact coatings with uniform the current density distribution are given in Table 1.

Table 1. The parameters of the PC regimes used in the electrodeposition processes and the thicknesses of coatings (t_c– deposition pulse, t_p– pause duration, ν– frequency, D_c– duty cycle, j_{av}– the average current density, j_A– the current density amplitude, and δ – thickness of coating).

No. of sample	t_c / ms	t_p / ms	ν / Hz	D_c / %	j_A / mA cm^{-2}	j_{av}/ mA cm^{-2}	δ / μm
1	5	28.3	30	15	100	15	40
2	5	15	50	25	100	25	40
3	5	7.5	80	40	100	40	40
4	5	5	100	50	100	50	40
5	5	5	100	50	80	40	40
6	5	5	100	50	120	60	40
7	5	5	100	50	100	50	10
8	5	5	100	50	100	50	20
9	5	5	100	50	100	50	60

The processes of electrodeposition were performed at a temperature of 22.0±0.50 ^oC in a cell of an open type. For a preparation of the electrolyte, p.a. reagents and ultra-pure water were used. The Si(111) orientation of (1.0 × 1.0) cm^2 surface area was used as a cathode. The preparation of Si(111) for electrodeposition was described elsewhere [18]. Copper in the form of plate was used as anode.

The Si(111) orientation was situated in the middle of square-shaped cell between two parallel Cu plates.

Morphological analysis of produced Cu coatings was performed by scanning electron microscope (SEM – model JEOL JSM-6610LV).

The preparation of the Cu coatings for analysis of internal structure was performed in the following way: process of revealing the geometry of the cross-section structure Si/Cr/Au/Cu started with a perpendicular cut of the Si wafers samples with electrodeposited Cu coatings. The samples were embedded in a self-curing methyl methacrylate-polymer (Palavit G, Heraeus, Germany) and mechanically polished with different SiC papers and alumina powder with different grain size (1 and 0.3 μm). Rinsing solution of Na_2CO_3 was used to avoid agglomeration of the alumina powder. Finally, the structures were dried in nitrogen flow.

Vickers microhardness measurements were performed at different applied loads, P (0.049–2.94 N) with constant (25 s) or variable dwell time (15–65 s) to study the mechanical features of the coatings. The number of different loads was 12. Indentation was performed at the room temperature. For a determination of hardness of coatings, the dwell time was 25 s. The indentation was made on a Vickers tester; model "Leitz Kleinert Prufer DURIMET I". The diagonals size of the indents were measured by optical microscope (Olympus CX41) connected to the computer with image software. The number of the indents was three and for calculation hardness we used arithmetic mean diagonal size. The optical microscopy image showing Vickers hardness indentation in the Cu coating obtained with D_c of 50 % (j_A = 100 mA cm^{-2}), an applied load of 0.49 N and a dwell time of 15 s is given in Fig. 1.

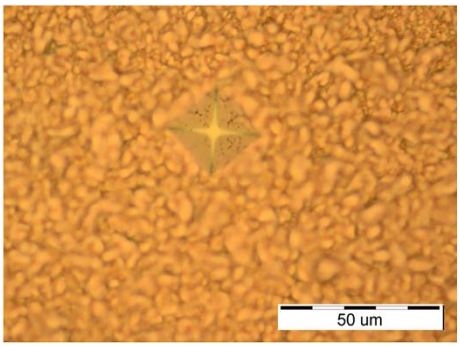

Figure 1. Vickers hardness indentation made by microhardness tester in the Cu coating obtained with D_c of 50 % (j_A = 100 mA cm^{-2}), an applied load of 0.49 N and a dwell time of 15 s. The thickness of coating: 60 μm.

The Chen-Gao mathematical composite hardness model was selected and applied to experimental data to obtain the true value of the coating hardness. Fitting of experimental data of diagonal size-composite hardness values was done in the Matlab software R2015a.

Indentation creep features of the Cu coatings were investigated by measurement of a hardness with a variation of dwell time (15–65 s) at fixed applied loads of P of 0.49 and 1.96 N at the room temperature.

Finally, Response Surface Methodology (RSM) predictive tool is applied for a purpose of predicting composite hardness of the Cu coatings. The correlation between input variables (duty cycle, coating thickness, and applied indentation loads) and measured output (composite hardness) was investigated. To establish the prediction model, RSM analysis in Design-Expert 12 software package (Stat-Ease, US) was used and Optimal (Custom) Design with 3 numerical factors and 4 levels is given in Table 2.

Table 2. Experimental range and level of the test variables used in the RSM analysis.

	Numerical factor	Units	levels	Range
A_1	Duty cycle	%	4	15–50
B_1	Thickness	μm	4	10–60
C_1	Applied load	N	4	0.1–1.5

3. RESULTS AND DISCUSSION

3.1. Basic facts

The duty cycle, D_c represents the ratio between the pulse duration and the period of a rectangular waveform, T_p as shown by Eq. (1) [38].

$$D_c = \frac{t_c}{T_p} \quad (1)$$

In Eq. (1), t_c is deposition pulse (or time), and D_c is commonly expressed in %.

The period of square wave pulsating is defined by Eq. (2):

$$T_p = t_c + t_p \quad (2)$$

where t_p is pause duration.

The duty cycle is related with a frequency of pulsating, ν by Eq. (3):

$$D_c = t_c \nu \quad (3)$$

since a frequency, ν is defined as:

$$\nu = \frac{1}{T_p} \quad (4)$$

The pulsating current (PC) regime is defined by Eq. (5) [6]:

$$j_{av} = j_A \frac{t_c}{t_c + t_p} \quad (5)$$

where j_{av} is the average current density and j_A is the current density amplitude.

Hence, it follows from Eqs. (1) and (5) that the average current density and duty cycle are related by Eq. (6):

$$j_{av} = j_A D_c \quad (6)$$

3.2. Morphological and internal structural analysis of the copper coatings obtained by various pulsating current (PC) regimes

Figure 2 shows SEM micrographs of copper coatings obtained with duty cycles of 15 (Fig. 2a), 25 (Fig. 2b), 40 (Fig. 2c) and 50 % (Fig. 2d). These duty cycles corresponded to frequencies of 30, 50, 80 and 100 Hz, respectively. The size of grains decreased, while compactness of the coatings increased with the increase of duty cycle. The larger grains of relatively regular shapes are obtained with duty cycles of 15 and 25 % (Fig. 2a and b). The fine-grained structures were obtained with duty cycles of 40 and 50 % (Fig. 2c and d).

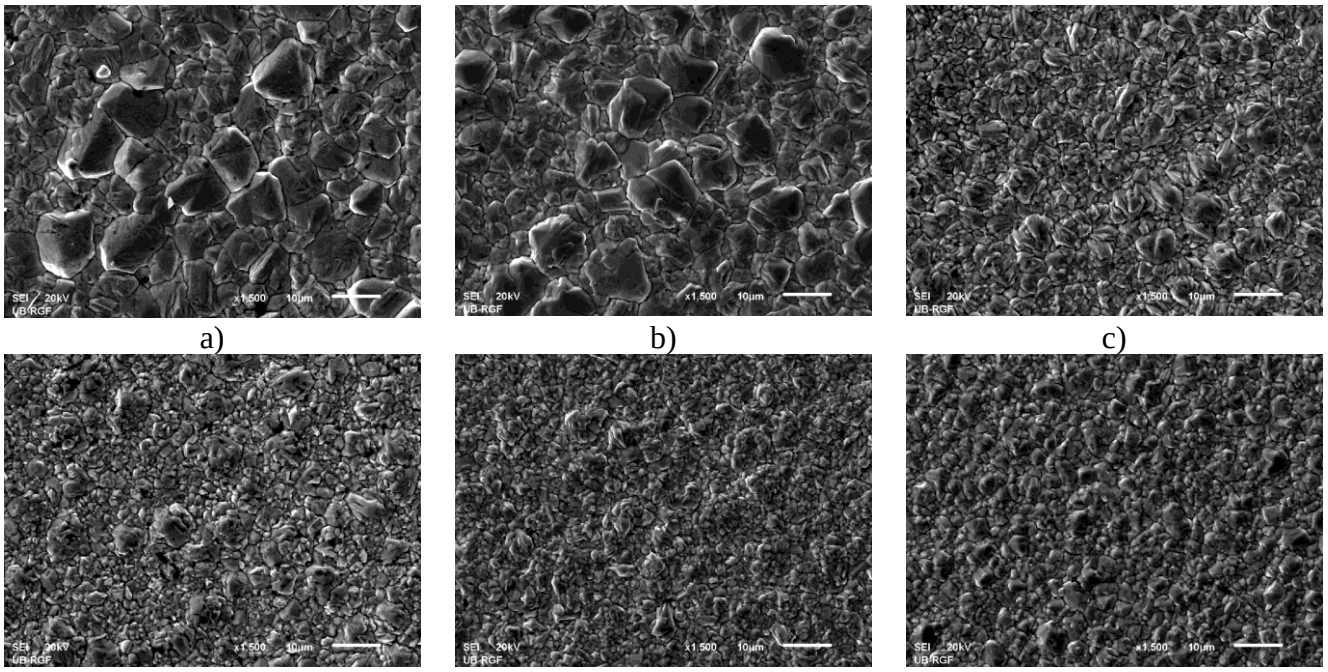

Figure 2. The Cu coatings obtained by various PC regimes: a) D_c = 15 %, b) D_c = 25 %, c) D_c = 40 %, d) D_c = 50 %; ((a)–(d): j_A = 100 mA cm^{-2}), e) D_c = 50 % (j_A = 80 mA cm^{-2}), and f) D_c = 50 % (j_A = 120 mA cm^{-2}). The thickness of the coatings: 40 μm.

The Cu coatings obtained with the same duty cycle (D_c = 50 %, or ν = 100 Hz), but with various the current density amplitudes, and hence, with various the average current densities are shown in Fig. 2e and f. At the first sight, it can be noticed that morphologies of the Cu coatings obtained with j_A of 80 mA cm^{-2} (Fig. 2e) and 120 mA cm^{-2} (Fig. 2f) were fine-grained and similar to those obtained with duty cycles of 40 % (Fig. 2c), and 50 % (Fig. 2d).

The decrease in size and regularity of grains with an increase of D_c can be ascribed to a decrease of contribution of activation control with simultaneous an increase of contribution of diffusion control in overall control of electrodeposition process [18]. Formation of large relatively regular grains with D_c of 15 and 25 % indicates the dominant effect of the activation control in the overall control of electrodeposition process; thereby a contribution of the activation control was larger

with D_c of 15 than with 25 %. With the further increase of D_c value, diffusion becomes a dominant process in the mixed activation-diffusion control of the electrodeposition, and as result of this, the fine-grained structures are formed with D_c of 50 %.

Formation of fine-grained structures with larger D_c values can be also explained following the basic nucleation law [6]: according to this law, nucleation rate increases with an increase of overpotential of electrodeposition. In our case, overpotential increases with an increase of the average current density [18], and consequently, with an increase of duty cycle (Table 1). Hence, a nucleation rate increases with an increase of duty cycle. This means that the larger number of nuclei is formed in the initial stage of electrodeposition growing simultaneously, and as a result of this, compact and uniform fine-grained structures are formed with the larger duty cycles.

The uniformity and compactness of formed Cu coatings can be confirmed by analysis of internal structure of the Cu coatings formed with various thicknesses (Fig. 3).

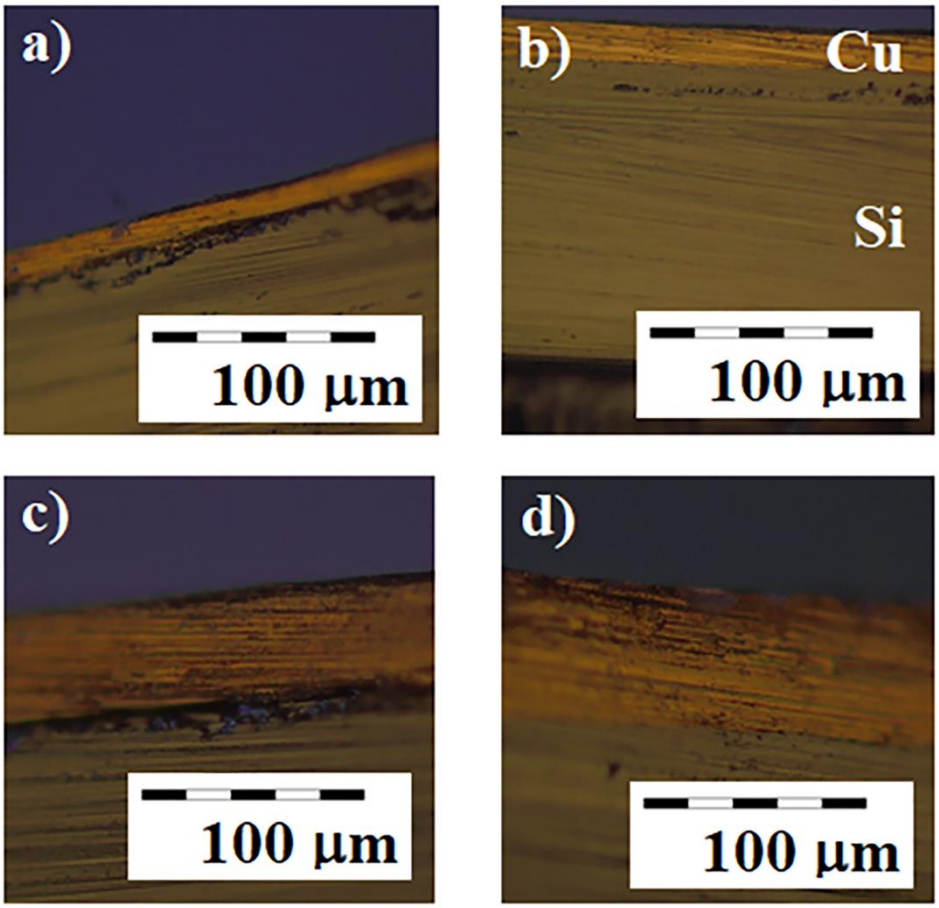

Figure 3. Cross section analysis of the Cu coatings obtained by the PC regime with D_c of 50 % (j_{av} = 50 mA cm^{-2} and j_A = 100 mA cm^{-2}), and thickness (δ) of: a) 10 µm, b) 20 µm, c) 40 µm, and d) 60 µm.

3.3. Theory of composite hardness model according to Chen–Gao (C–G)

A mixed composite hardness model, Chen-Gao (C–G), was selected to analyze the absolute hardness of the copper coatings. Mixed composite hardness model (united *area low of mixture* and *volume low of mixtures)* expresses a composite hardness as sum of all contributions from different indentation depths, and composite hardness is proportional to two factors. The first factor is the intrinsic hardness of the local material, *H(h)*, and the second one is a weight function, *p(h)* [29–31].

The C–G method introduces composite hardness as a function of critical reduced depth beyond which a material will have no effect on the measured hardness. The critical reduced depth, *b* represents ratio between a radius of plastic zone beneath the indentation and the indentation depth. The correlation between a composite hardness value, H_c and the critical reduced depth, *b* is given by Eq. (7):

$$H_c = H_s + \left[\frac{m+1}{m \cdot b} \cdot \frac{\delta}{h} - \frac{1}{m \cdot b^{m+1}} \cdot \frac{\delta^{m+1}}{h^{m+1}}\right] \cdot \left(H_{coat} - H_s\right) \quad (7)$$

where H_s and H_{coat} are hardness of the substrate and the coating, respectively, δ is coating thickness, *h* is an indentation depth and *m* is the power index. The convenient value for *m* is found to be 1.8 for "soft film on hard substrate" and *m* = 1.2 for "hard film on soft substrate". The used *m* value is intermediate between that predicted by assuming an *area low of mixtures* (*m* = 1) and a *volume low of mixtures* (*m* = 2) [39].

Equation used to fit the composite hardness as a function of depth is given in the form:

$$H_c = A + B \cdot \frac{1}{h} + C \cdot \frac{1}{h^{m+1}} \quad (8)$$

where *A*, *B* and *C* are fitting parameters used to calculate the absolute hardness of film (or coating). Then, the absolute hardness is calculated using Eq. (9):

$$H_{coat} = A \pm \sqrt[m]{\frac{\left[m \cdot |B| / (m+1)\right]^{m+1}}{m \cdot |C|}} \quad (9)$$

In Eq. (8), an indentation depth, *h*, can be replaced with a diagonal size (there is a linear relation between *h* and *d* in the form *h* = *d*/7). In Eq. (9), the sign "+" is used for "hard film–soft substrate" system, and the sign "–" is used for "soft film–hard substrate" system [29–31, 39]. The diagonal, *d*, was measured directly on the Cu coating after an indentation, and then, composite Vicker's hardness was calculated according to Eq. (10):

$$H_c = \frac{2 \cdot P \cdot \sin\left(\frac{\theta}{2}\right)}{d^2} = 0.01854 \cdot \frac{P}{d^2} \quad (10)$$

where *P* is the load force applied to the indenter (in N) and θ is an angle between opposite faces of the diamond squared pyramid indenter [40].

3.3.1. Hardness analysis of the Cu coatings

Due to a high hardness Si(111) substrate of 7.42 GPa [18], the Cu coatings on Si(111) belong to "soft film on hard substrate" type of composite systems. The Chen-Gao model is applied for a determination of hardness of the Cu coatings, because this model was just proposed for this type of the composite systems [29–31]. The model is originally developed for the coating of Cu obtained by sputtering on glass [30], and according to our knowledge, there is no relevant data in its application for electrolytically obtained coatings.

The dependencies of the composite hardness of the Cu coatings on indentation depth, h calculated by Eq. (10) for various duty cycles, the current density amplitudes and the thickness of coatings are shown in Fig. 4.

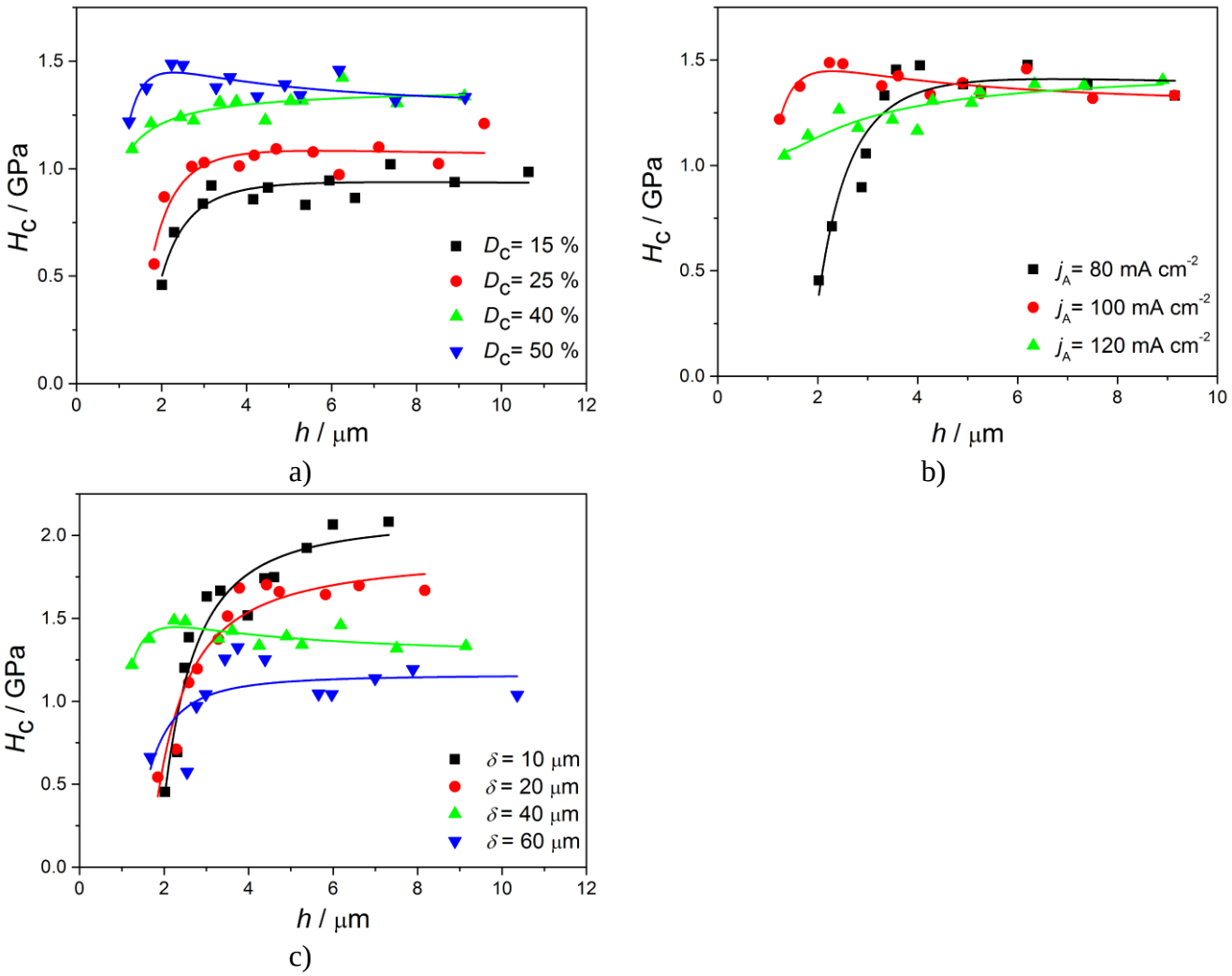

Figure 4. The dependencies of the composite hardness of the Cu coatings, H_c on indentation depth, h calculated by Eq. (10) for various: a) duty cycles, b) the current density amplitudes, and c) the thickness of coatings.

Please note that the dependencies obtained with D_c of 50 % (Fig. 4a), j_A of 100 mA cm^{-2} (Fig. 4b) and δ of 40 μm (Fig. 4c) are of the same Cu coating (Table 1).

The parameters *A*, *B* and *C* obtained by fitting of Eq. (8) and calculated hardness of the Cu coatings according to the Eq. (9) are given in Table 3.

Table 3. Fitting parameters of the Chen-Gao composite hardness model with calculated hardness (H_{coat}) for all Cu coatings, parameters (*A, B, C*) and error fitting (*RMSE* – Root Mean Square Error).

	D_c / %	j_A/ mA cm^{-2}	δ / μm	H_{coat} /GPa	*A*	*B*	*C*	*RMSE*
1	15	100	40	0.9069	0.914	1.966	–907.4	0.006436
2	25	100	40	1.0261	1.035	2.97	–812.8	0.07438
3	40	100	40	1.3136	1.379	–2.234	–16.94	0.04728
4	50	100	40	1.5079	1.533	–8.312	353	0.05442
5	50	80	40	1.3164	1.324	6.316	–2313	0.11882
6	50	120	40	1.4367	1.459	4.684	–245.7	0.04889
7	50	100	10	2.119	2.119	–4.019	–2317	0.1573
8	50	100	20	1.914	1.914	–7.587	–1176	0.1209
9	50	100	60	1.164	1.164	–0.7037	–503.1	0.1845

The coating hardness increased from 0.9069 to 1.5079 GPa with an increase of duty cycle, D_c from 15 to 50 %, i.e. with an increase of j_{av} from 15 to 50 mA cm^{-2}, and ν from 30 to 100 Hz (Table 3). All these Cu coatings were obtained with j_A of 100 mA cm^{-2}. Hence, the maximum hardness was obtained for the coating produced with D_c of 50 %, j_{av} of 50 mA cm^{-2} and j_A of 100 mA cm^{-2}.

Comparing the Cu coatings obtained with the same D_c of 50 % (i.e. with ν of 100 Hz), but with different j_A values (80, 100 and 120 mA cm^{-2}), the maximum hardness showed the coating obtained with j_A of 100 mA cm^{-2}. Although all three Cu coatings were fine-grained, the smaller hardness of the Cu coating obtained with j_A value of 120 mA cm^{-2} than that obtained with j_A of 100 mA cm^{-2} can be ascribed to the increase of the effect of diffusion with increasing the current density amplitude value [18].

The increase of hardness of the Cu coatings with increasing the duty cycles can be correlated with morphology of the coatings as follows: plastic deformation in Cu coatings is determined by either dislocation propagation inside the Cu grains or grain boundary sliding [41, 42]. With decreasing the grain size, it increases the number of grain boundaries acting as disruption sites for dislocation motion and grain boundary sliding becomes dominant process causing the larger hardness of the Cu coatings with smaller size of the grains. Also, the large number of stacking faults in the grains can also contribute to hardness of the coatings, because intragranular nanotwins hinder dislocation propagation in a similar way as high-angle grain boundaries [43].

Analyzing the effect of the thickness of coating on their hardness, the Cu coating of 10 μm thickness showed the largest hardness, with a tendency of decrease of hardness with increasing the thickness of coating. Furthermore, the Cu coating of this thickness had the largest hardness from all analyzed coatings. This can be ascribed to a high contribution of substrate hardness to measured

composite hardness, and consequently, to absolute hardness of the coating. It was shown recently [18] that a thickness of 40 μm is optimum for which a contribution of Si(111) as very hard substrate is eliminated. Simultaneously, the roughness of coatings increased noticeably with increasing the coating thickness [18], making also a significant effect on the coating hardness.

The obtained values of coatings hardness are in an excellent agreement with those found in the literatures for electrolitically produced Cu coatings. The composite hardness of Cu coatings strongly depends on working conditions and regimes of electrodeposition, as well as of applied composite hardness models. Depending on a type of electrolyte, applied current density, type of substrate, thickness of electrodeposited coating, the presence of additives, mixing of electrolyte, applied load, etc. the usual values of coating hardness obtained by application of constant galvanostatic (DC) regime are in the 0.70–1.65 GPa range [8, 44, 45]. For example, the Cu coating hardness determined by Korsunsky model was 0.80 GPa [39]. The values of composite hardness of the Cu coatings obtained by application of various pulse reverse regimes of electrodeposition are in the 1.10–2.0 GPa range, and they were slightly higher than those obtained in the DC regimes [9]. Anyway, comparable values of the coating hardness obtained in this investigation by application of Chen-Gao model with those found in the literatures clearly indicate that the Cheng-Gao model can be successfully used for a determination of hardness of the Cu coatings obtained by various electrodeposition processes.

Although the values obtained by application of various composite hardness models cannot be mutually compared, the trend of change of coating hardness observed by application of the Cheng-Gao model was equivaltent to recently observed trend achieved by application of Chico-Lesage model for the same Cu coatings [18]. This can be additional proof of succsessfull implementation of the Cheng-Gao model for hardness analysis of electrolytically produced Cu coatings.

3.4 Indentation creep analysis of the Cu coatings

Microsystem devices need to hold their mechanical integrity for long-term exploitation. The indentation creep testing is very useful non-destructive technique for assessment the creep behavior of the materials. The results of hardness measurements were used for the creep mechanism specification through calculation the stress exponent μ of the coatings according to the model of Sargent-Ashby [46]. Eq. (11) gives the relation between the time-dependent composite hardness H_c and stress exponent μ as:

$$H_c = \frac{\sigma_0}{\left(c \cdot \mu \cdot \varepsilon_0 \cdot t\right)^{\frac{1}{\mu}}} \qquad (11)$$

where ε_0 is the strain rate at reference stress σ_0, c is constant, t is dwell time and μ is the stress exponent.

The plots of $\ln H_c$ against $\ln t$ give straight lines whose slopes are equivalent to the negative inverse stress exponent ($-1/\mu$). The value of the stress exponent, μ, may be considered as the indicator of the mechanism affecting the deformation. If its value is around 1, a diffusion creep was happened. If the value of μ is around 2 the creep mechanism is a grain boundary sliding. With further increasing its

value (in the range between 3 and 10), mechanism of deformation will be dislocation climbs and dislocation creep [47, 48].

Indentation creep tests were performed on all the Cu coatings obtained by the PC regimes with variation of the electrodeposition parameters: the duty cycle (15, 25, 40 and 50 %), the current density amplitude (80, 100 and 120 mA cm^{-2}) and the coating thicknesses (10, 20, 40 and 60 μm).

The dwell time was chosen to be in range of 15 to 65 s, in increments of 10 s. At these moments, the indentation diagonals were measured and the values of the composite hardness were calculated. Indentation results are expressed as variation of the composite hardness H_c with a dwell time (t) at the applied load of 0.49 N for samples obtained with different the duty cycles (Fig. 5a), the current density amplitudes (Fig. 5b) and the coating thicknesses (Fig. 5c). The similar to Fig. 4, variations observed with D_c of 50 % (Figs. 5a and 6a), j_A of 100 mA cm^{-2} (Figs. 5b and 6b) and δ of 40 μm (Figs. 5c and 6c) belong to the same Cu coating.

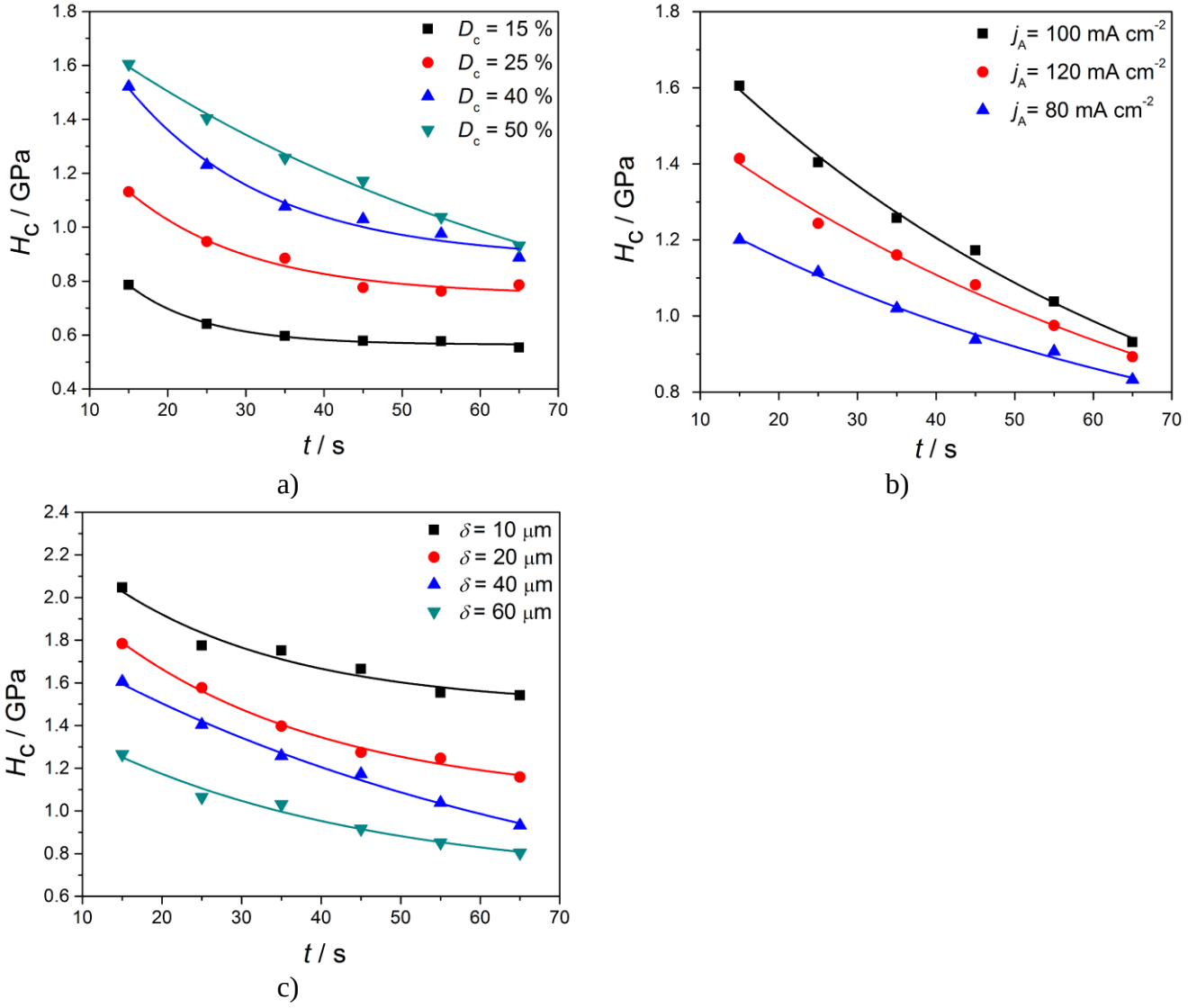

Figure 5. Variation of the composite hardness of the Cu coatings as a function of dwell time at constant load 0.49 N for various: a) the duty cycles, b) the current density amplitudes, and c) the thickness of coatings.

Indentation experiments have shown that a further increase in depth occurs over time at the same maintained load which means that the composite hardness decreases with increase of the dwell time.

Figure 6 shows the experimental data of composite hardness variation with dwell time fitted according to Sargent-Ashby model in order to determine the stress exponent μ. Stress exponent values are expected to indicate dependence of the creep behavior on the coating microstructure.

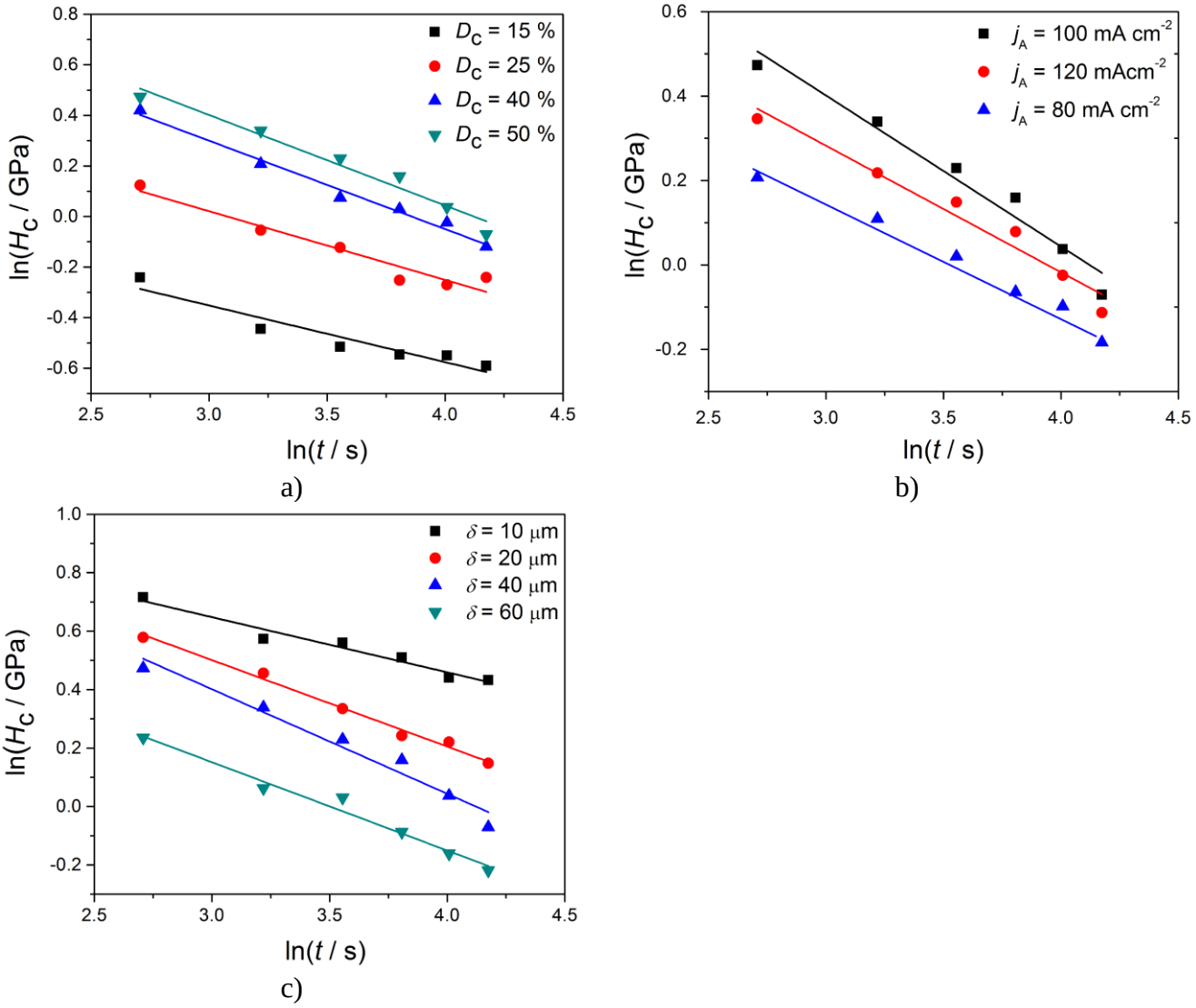

Figure 6. Variation of lnH_c against ln$t$ at the load 0.49 N for various: a) duty cycles, b) the current density amplitudes, and c) the thickness of coatings.

Variation of lnH_c against ln$t$ at applied load 0.49 N for duty cycles of 15, 25, 40 and 50 % is given on Fig 6a, for 80, 100 and 120 mA cm^{-2} the current density amplitudes on Fig. 6b and for 10, 20, 40 and 60 μm thickness of the coatings on Fig. 6c.

The values of the estimated stress exponent μ for all the coatings are given in Table 4.

Table 4. Fitting results and stress exponents for the Cu coatings obtained by the PC regimes with various the duty cycles, the current density amplitudes and the coatings thickness at a constant load 0.49 N.

The parameters of the PC regimes	Slope (k)	Intercept (n)	Stress exponent (μ)
D_c / %[1]			
15	–0.2240	0.3201	4.46
25	–0.2556	0.7946	3.91
40	–0.3495	1.3483	2.86
50	–0.3579	1.4751	2.79
j_A / mA cm^{-2}[2]			
80	–0.2612	0. 9328	3.83
100	–0.3579	1.4751	2.79
120	–0.3000	1.1824	3.33
δ / μm[3]			
10	–0.1889	1.2146	5.29
20	–0.2959	1.3889	3.38
40	–0.3579	1.4751	2.79
60	–0.3024	1.059	3.31

In this investigation, the values of the stress exponent, μ, obtained at the load 0.49 N, ranging from 2.79 to 5.29. The value of this exponent increases with decreasing duty cycle. Regarding the values obtained for various the current density amplitudes, the lowest stress exponent has the Cu coating obtained with j_A of 100 mA cm^{-2}. As far as the values obtained for various the coatings thickness, the highest value of the stress exponent, μ of 5.29 is obtained for 10 μm thick Cu coating. This high value clearly indicates the effect of a very hard Si substrate must also be included in preventing the creep process.

The obtained values are in a good agreement with morphology of the coatings obtained under the given electrodeposition conditions, as well as with the values of coating hardness calculated according to the C-G model. The lowest value of the stress exponent (μ = 2.79) corresponds to Cu coating with fine-grained structure obtained with D_c of 50 %, j_A of 100 mA cm^{-2} and δ of 40 μm (Fig. 2d). Simultaneously, this Cu coating showed the highest value of the coating hardness (H_{coat} = 1.5079 GPa). The other coatings with fine-grained structures (Fig. 2c, e and f) and with the high values of the coating hardness among 1.3136 and 1.4367 GPa had the stress exponents larger than 2.79, but less than 4. The stress exponent increases with increasing the size of grains, and this exponent was 4.46 for the coating characterized by large and relatively regular grains obtained with D_c of 15 % (Fig. 2a). This Cu coating had the lowest coating hardness of 0.9069 GPa.

According to Ref. [48], the obtained stress exponents between 2.79 and 5.29 correspond to the creep mechanisms named the grain boundary sliding, the dislocation climbs and the dislocation creep, with a tendency of the change of creep mechanism from grain boundary sliding to dislocation climbs

[1] In all experiments: j_A = 100 mA cm^{-2}, and δ = 40 μm
[2] In all experiments: D_c = 50 %, and δ = 40 μm
[3] In all experiments: j_A = 100 mA cm^{-2}, and D_c = 50 %.

and dislocation creep with increasing the stress exponent. For the Cu coating obtained with D_c of 50 % and j_A of 100 mA cm^{-2}, the μ value of 2.79 indicates that the dominant creep mechanism is the grain boundary sliding. This is in excellent agreement with the high hardness of this Cu coating, where the high hardness is determined by fine-grained structure with numerous grain boundaries representing disruption sites for dislocation motion [41]. On the contrary, the high μ exponent of 4.46 obtained for the Cu coating produced with D_c of 15 % which is characterized by large and relatively well defined grains indicated that the dominant mechanism is related with dislocation phenomena. As a result of this, the hardness of the coatings with dominant dislocation mechanisms is considerably smaller than that with dominant grain boundary sliding.

According to the power low creep, the decrease of the stress exponent corresponds to the increase in creep rate and it can be seen from Fig. 5, especially from Fig. 5a, for D_c of 40 and 50 %. The coatings with the higher value of the stress exponent are more resistant to creep caused by indentation at low loads.

Two indentation creep tests were additionally performed on the coatings obtained with D_c of 25 and 50 % at the higher load of 1.96 N than previously analyzed (0.49 N load) and the results are shown in Fig. 7.

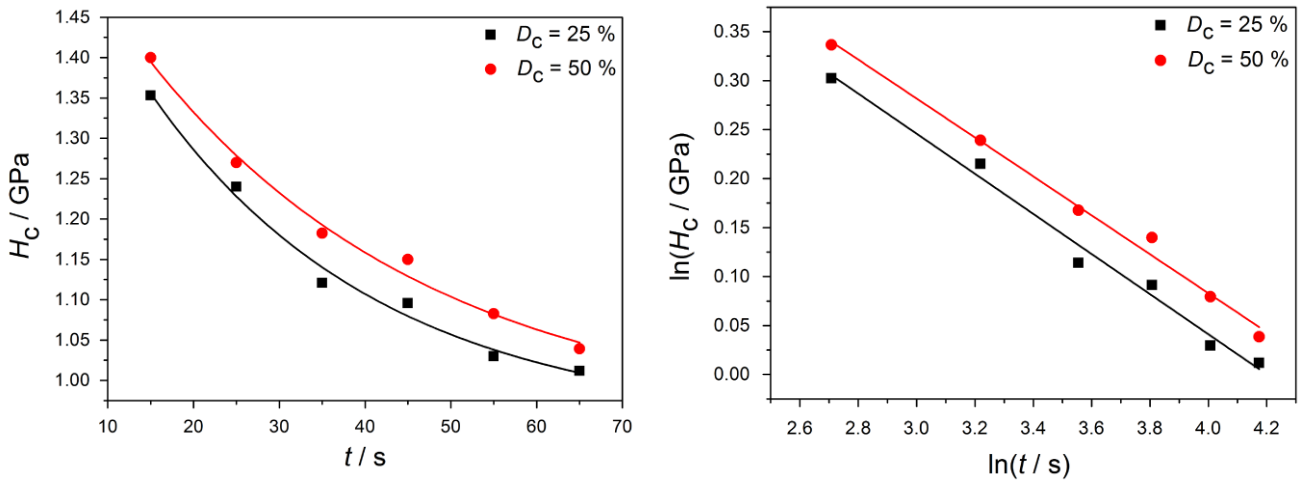

Figure 7. Variation of: a) the composite hardness of the Cu coatings as a function of dwell time, and b) lnH_c against ln$t$, at constant load 1.96 N for duty cycles of 25 and 50 %.

It can be seen that the indentation creep mechanism changes with increasing load and that creep is less sensitive to the electrodeposition parameters and the coating microstructure at high loads. This can be inferred from the values of the stress exponent. For the coating formed with D_c of 25 %, the stress exponent, μ was 3.91 at a load of 0.49 N and 4.88 at a load of 1.96 N. For the coating obtained with D_c of 50 %, the stress exponent, μ was 2.79 at a load of 0.49 N and 5.03 at a load of 1.96 N.

By comparing the differences in the value of the stress exponent for the fine-grained coatings (D_c = 50 %, j_A = 100 mA cm^{-2}) and the coarse-grained coatings (D_c = 25 %, j_A = 100 mA cm^{-2}) at 0.49 N and 1.96 N, it can be seen that the value of the exponent change is almost double for the coatings

with fine-grained microstructure, *i.e.* the Cu coatings with fine-grained microstructure are more sensitive to creep, especially at the low loads.

3.5. Predictive modeling of composite hardness values by application of Response Surface Methodology (RSM)

Using data given in Table 2, a regression model related to response of the variables for prediction of the composite hardness value was developed. The relationship enabling a prediction of the composite hardness (H_c) values of the Cu coatings in a function of applied variables (duty cycle (D_c), thickness of the coating (δ) and indentation load (P)) is given by Eq. (12):

$$H_c = 1.28 + 0.1715 \cdot A_1 - 0.1928 \cdot B_1 + 0.2278 \cdot C_1 + 0.2003 \cdot A_1 \cdot B_1 + 0.1354 \cdot A_1 \cdot C_1 - 0.1816 \cdot B_1 \cdot C_1 - 0.1870 \cdot A_1^2 - 0.1333 \cdot B_1^2 - 0.0647 \cdot C_1^2 \quad (12)$$

where A_1, B_1 and C_1 represent numerical factors from Table 2 corresponding to the input variables, i.e. duty cycle, applied load and the thickness of coating.

The corresponding 3D (three dimensional) surface plots showing the dependence of H_c values predicted by application of the Response Surface Methodology (RSM) based on the regression model generated by Eq. (12) on duty cycle, thickness of coating and applied load are shown in Fig. 8.

It can be seen from Fig. 8 that the duty cycle achieved a significant effect on the composite hardness value. For an applied load of 1 N and a 40 μm thickness of the coating, the composite hardness increased from 0.865 to 1.34 GPa with an increase of duty cycle from 15 to 50 %. In a similar way, the composite hardness increased with the increasing applied load from 0.1 to 1.5 N (Fig. 8b). The effect of substrate hardness on the composite hardness is dominant at small thickness of coatings while for a high load, this effect gradually decreases with increasing the thickness of coating (Fig. 8c).

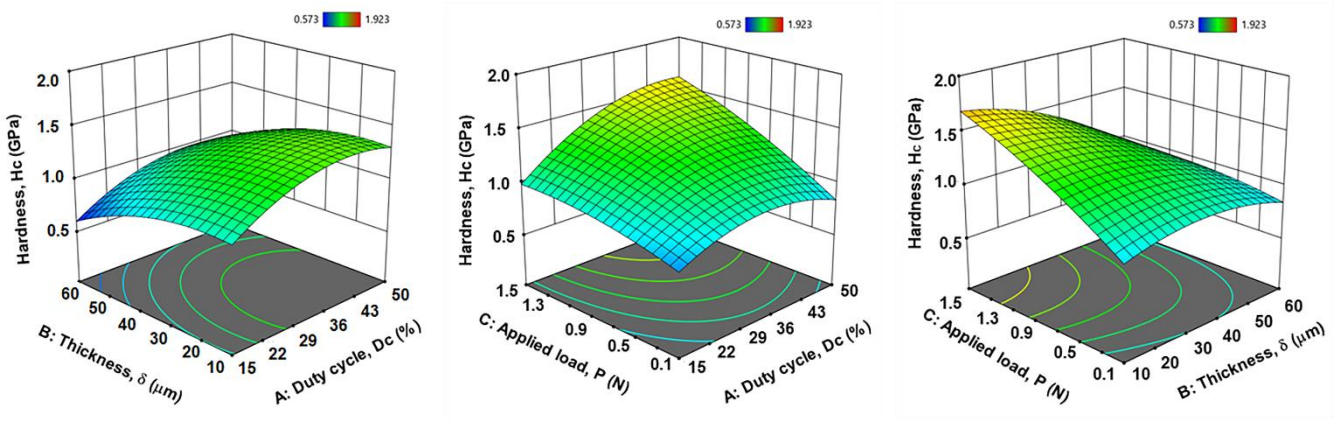

a) b) c)

Figure 8. The response surface plot of the composite hardness prediction as the function: a) duty cycle and the thickness of coatings, b) duty cycle and applied load, and c) applied load and the thickness of coatings.

The optimal parameters obtained through application of RSM were: duty cycle (D_c): 44.33 %, applied load (P): 0.98 N, thickness of the coating (δ): 43.38 μm and the composite hardness (H_c): 1.457 GPa. If the optimization criterion is a minimal composite hardness value, solution parameters were: D_c = 15.12 %, δ = 59.50 μm, P =1.05 N and H_c = 0.57 GPa.

It was found that the composite hardness is predicted by application of the regression model with a maximum error of 3.2 %. The values of probability which were less than 0.050 and determination coefficient (R^2) evaluating correlation between experimental and predicted values of 0.90 clearly indicate that this model is successfully applied. The attained excellent agreement between these two kinds of values of the composite hardness shows that the RSM represent a suitable tool for optimization of the electrodeposition processes with the aim to obtain coatings of desired characteristics, in this case, hardness.

4. CONCLUSIONS

Copper coatings were formed by electrodeposition on Si(111) substrate using the pulsating current (PC) regime by varying either duty cycle (i.e. the average current density or frequency for the same current density amplitude) or the current density amplitude (for the same duty cycle). Morphology and internal structure were examined by the scanning electron microscope (SEM) and optical microscope (OM), respectively. The hardness and indentation creep features of the Cu coatings were analyzed from the mechanical features. The Response Surface Methodology (RSM) was used for optimization of process formation and mechanical features of the Cu coatings. On the basis of the obtained results, it follows:

- The regularity and size of Cu grains decreased with an increase of duty cycle from 15 to 50 %. The fine-grained structures are formed with a duty cycle of 50 %. Irrespective of the thickness of coating, analysis of the internal structure showed formation of compact and uniform coatings with a duty cycle of 50 %.
- The hardness of the Cu coatings was determined by applying the Chen-Gao (C-G) composite hardness model and the obtained values in the range (0.9069–1.5079) GPa indicated the succsesfull implementation of this model in determination of true hardness of Cu coatings. The maximum hardness showed the Cu coating with fine-grained structure obtained with a duty cycle of 50 % and the current density amplitude of 100 mA cm^{-2}.
- The stress exponents in the (2.79–5.29) range were obtained by indentation creep analysis of the Cu coatings, and the value of this exponent increased with decreasing the duty cycle. The lowest value of this exponent of 2.79 was obtained for the Cu coating with the maximum hardness, proving that deformation of the coating during microindentation is determined by grain boundary sliding.
- Using Response Surface Methodology (RSM), optimization of process of formation of the Cu coatings by the PC regime and the hardness was considered, and the obtained error of 3.2 % indicated the good agreement between predicted and experimentally obtained values.

ACKNOWLEDGEMENT
This work was financially supported by the Ministry of Education, Science and Technological Development of the Republic of Serbia (Grants No. 451-03-68/2020-14/200026 and 451-03-68/2020-14/200135).

References

1. M. Cortés, S. Martínez, C. Serre, E. Gómez, A. Pérez-Rodríguez and E. Vallés, *Sens. Actuators B*, 173 (2012) 737.
2. E. Delbos, L. Omnès and A. Etcheberry, *Microelectron. Eng.*, 87 (2010) 514.
3. I. Mladenović, Z. Jakšić, M. Obradov, S. Vuković, G. Isić, D. Tanasković and J. Lamovec, *Opt. Quantum Electron.*, 50 (2018) 203.
4. G. Frost and L. Ladani, *J. Electron. Mater.*, 49 (2020) 1387.
5. J. F. Rohan and D. Thompson, Frontiers of Cu Electrodeposition and Electroless plating for On-chip Interconnects. In *Copper Electrodeposition for nanofabrication of Electronics Devices*, K. Kondo, R. N. Alkolkar, D. P. Barkey and M. Yokoi (Eds.), Springer, New York, 2014, 171, 99–101.
6. K. I. Popov, S. S. Djokić, N. D. Nikolić and V. D. Jović, *Morphology of Electrochemically and Chemically Deposited Metals*, Springer International Publishing, (2016) New York, USA.
7. C.-F. Chen and K.-C. Lin, *Jpn. J. Appl. Phys.*, 41 **(**2002) 2881.
8. L. Martins, J. I. Martins, A. S. Romeira, M. E. V. Costa, J. D. M. Costa and M. Bazzaoui, *Mater. Sci. Forum*, 455–456 (2004) 844.
9. P. Kristof and M. Pritzker, *Plat. Surf. Finish*., (1999) 237.
10. A. Mallik and B. C. Ray, *Thin Solid Films*, 517 (2009) 6612.
11. N. Tantavichet and M. D. Pritzker, *Electrochim. Acta*, 50 (2005) 1849.
12. J. Ni, K. Han, M. Yu, C. Zhang, *Int. J. Electrochem. Sci.*, 12 (2017) 6874.
13. H. Fan, S. Cao, Y. Zhao, S. Wang, *Int. J. Electrochem. Sci.*, 14 (2019) 8256.
14. R. Sekar, *Trans. Nonferrous Met. Soc. China*, 27 (2017) 1665.
15. R. Seakr, *Trans. Nonferrous Met. Soc. China*, 27 (2017) 1423.
16. N. N. C. Isa, Y. Mohd, M. H. M. Zaki and S. A. S. Mohamad, *Int. J. Electrochem. Sci.*, 12 (2017) 6010.
17. I. Mladenović, J. Lamovec, V. Jović, M. Obradov, D. Vasiljević-Radović, N.D. Nikolić and V. Radojević, *J. Serb. Chem. Soc.*, 84 (2019) 729.
18. I. O. Mladenović, J. S. Lamovec, D. G. Vasiljević-Radović, R. Vasilić, V. J. Radojević and N. D. Nikolić, *Metals*, 10 (2020) 488.
19. J. Malzbender, J. M. J. Toonder, A. R. Balkenende and G. With, *Mater. Sci. Eng. R*, 36 (2002) 47.
20. S. J. Bull, *Thin Solid Films*, 688 (2019) 137452.
21. P. J. Burnett and D. S. Rickerby, *Thin Solid Films*, 148 (1987) 51.
22. J. Lesage and D. Chicot, *Surf. Coat. Technol.*, 200 (2005) 886.
23. A. M. Korsunsky, M. R. McGurk, S. J. Bull and T. F. Page, *Surf. Coat. Technol.*, 99 (1998) 171.
24. D. Beegan and M. T. Laugier, *Surf. Coat. Technol.*, 199 (2005) 32.
25. D. Devaraj and S. K. Seshadri, *Plat. Surf. Finish.*, (1992) 72.
26. M. Hakamada, Y. Nakamoto, H. Matsumoto, H. Iwasaki, Y. Chen, H. Kusuda and M. Mabuchi, *Mater. Sci. Eng. A*, 457 (2007) 120.
27. A. Augustin, P. Huilgol, K. R. Udupa and K. U. Bhat, *J. Mech. Behav. Biomed. Mater.*, 63 (2016) 352.
28. J. Lesage, A. Pertuz, E. S. Puchi-Cabrera and D. Chicot, *Thin Solid Films*, 497 (2006) 232.
29. M. Chen and J. Gao, *Mod. Phys. Lett. B*, 14 (2000) 103.

30. J. L. He, W. Z. Li and H. D. Li, *Appl. Phys. Lett.*, 69 (1996) 1402.
31. Q. Hou, J. Gao and S. Li, *Eur. Phys. J. B*, 8 (1999) 493.
32. T. Chudoba and F. Richter, *Surf. Coat. Technol.*, 148 (2001) 191.
33. M. Y. Soomro, I. Hussain, N. Bano, E. Broitman, O. Nur and M. Willander, *Nanoscale Res. Lett.*, 7 (2012) 146.
34. P. H. Lin, X. H. Du, Y. H. Chen, H. C. Chen and J. C. Huang, *AIP Adv.*, 6 (2016) 095125.
35. W. Li, B. Yu, J. Tam, J. D. Giallonardo, D. Doyle, D. Poirier, J. G. Legoux, P. Lin, G. Palumbo and U. Erb, *J. Nucl. Mater.*, 532 (2020) 152039.
36. G. Orhan, G. Hapcy and O. Keles, *Int. J. Electrochem. Sci.*, 6 (2011) 3966.
37. N. V. Ponraj, A. Azhagurajan, S. C. Vettivel, S. X. Shajan, P. Y. Nabhiraj and A. Haiterlenin, *Met. Sci. Heat Treat.*, 60 (2019) 61.
38. N. Ghamarian, Z. Zainal, M. Zidan and W. T. Tan, *Int. J. Electrochem. Sci.*, 8 (2013) 312.
39. L. Magagnin, R. Maboudian and C. Carraro, *Thin Solid Films*, 434 (2003) 100.
40. J. J Gilman, *Hardness-a Strength Microprobe, Ch. 4 of The Science of Hardness Testing and Its research Applications*, J. H. Westbrook and H. Conrad, (Eds.) Ohio, USA: American Society of Metal, Metal Park, 1973.
41. A. Varea, E. Pellicer, S. Pané, B. J. Nelson, S. Suriñach, M. D. Baró and J. Sort, *Int. J. Electrochem. Sci.*, 7 (2012) 1288.
42. H. Zhang, Z. Jiang and Y. Qiang, *Mater. Sci. Eng. A*, 517 (2009) 316.
43. X. Zhang, A. Misra, H. Wang, M. Nastasi, J. D. Embury, T. E. Mitchell, R. G. Hoagland and J. P. Hirth, *Appl. Phys. Lett.*, 84 (2004) 1096.
44. A. A. Kasach, I. I. Kurilo, D. S. Kharitonov, S. L. Radchenko and I. M. Zharskii, *Russ. J. Appl. Chem.*, 91 (2018) 207.
45. S. Tao and D Y Li, *Nanotechnology*, 17 (2006) 65.
46. P. M. Sargent and M. F. Ashby, *Mater. Sci. Technol.*, 8 (1992) 594.
47. S. Farhat, M. Rekaby and R. Awad, *SN Appl. Sci.*, 1 (2019) 546.
48. B. Walser and O. D. Sherby, *Scr. Metall.*, 16 (1982) 213.